



## Copyright Notice

©2008 IEEE. Personal use of this material is permitted. However, permission to reprint/republish this material for advertising or promotional purposes or for creating new collective works for resale or redistribution to servers or lists, or to reuse any copyrighted component of this work in other works must be obtained from the IEEE.

This document was downloaded from Chalmers Publication Library (<http://publications.lib.chalmers.se/>), where it is available in accordance with the IEEE PSPB Operations Manual, amended 19 Nov. 2010, Sec. 8.1.9 (<http://www.ieee.org/documents/opsmanual.pdf>)

(Article begins on next page)

# On the Design of Interleavers for BICM Transmission

Alex Alvarado, Leszek Szczecinski<sup>§</sup>, Erik Agrell, and Arne Svensson

Department of Signals and Systems, Communication Systems Group

Chalmers University of Technology, Gothenburg, Sweden

<sup>§</sup>INRS-EMT, University of Quebec, Montreal, Canada

{alex.alvarado,agrell,arnes}@chalmers.se, leszek@emt.inrs.ca

**Abstract**—In this paper we design interleavers for bit-interleaved coded modulation (BICM) based on popular convolutional codes and quadrature amplitude modulation with Gray mapping. We analyze the so-called *modular interleavers* where the outputs of the convolutional encoder are appropriately matched with the input bits of the modulator. To quantify the achievable improvements we develop bounds on the coded BER using the multidimensional weight distribution spectrum of a code together with an equivalent QAM channel model. Based on these bounds, we show that the assignment of the encoder's output to the bit positions in the symbol significantly affects the system performance. The analytical developments are contrasted with numerical simulations. The improvements obtained through the proposed approach do not change the receiver's complexity and, depending on the system's parameters (rate, modulation, code's memory), they may be up to 1.7 dB!

**Index Terms**—BER, BICM, Convolutional Codes, Gray Mapping, QAM, Modular Interleaver, Random Interleaver, Union Bound

## I. INTRODUCTION

Bit-interleaved coded modulation (BICM) [1], [2] is a flexible modulation/coding scheme where the output of the channel encoder and the input to the modulator are separated by a (pseudo)random bit-level interleaver. At the receiver's side, the reliability metrics are calculated for the coded bits in the form of logarithmic likelihood ratios, or simply *L-values*. These metrics are then deinterleaved and further used by the soft-input channel decoder.

Following the framework set in [2], (pseudo)random (RN) interleavers are most often applied. This simplifies the analysis of the resulting BICM systems but leads to sub-optimality already noted in the literature. For example, [1] postulated the application of independent interleavers between each of the encoder's output and the corresponding modulator's input (e.g., using three interleavers for a 2/3-rate encoder, each of them feeding bits to one of the bits' positions in the 8-PSK symbol). A similar scheme was proposed in [3] where the idea of BICM with iterative demapping was introduced. In [4] similar modular (MD) interleavers—called there “in-line” interleavers—were proposed in the context of serially concatenated systems. When such MD interleavers are used, the performance gains will strongly depend on the bit assignment

between the encoder's output and the (unequally protected) bit positions in the complex symbol. Interleaver design for turbo coded BICM has been analyzed in [5] where a greedy design algorithm was proposed, and in [6] for BICM with low-density parity-check (LDPC) codes.

Performance evaluation of BICM for high-order modulations was usually limited by the lack of formal description of the metrics used in the decision process. This problem was partially solved by bounding techniques, e.g., [1] or the so-called expurgated bounds in [2]. However, these techniques are either very loose, or when tight, they must be algorithmic.

In this paper we use the results presented in [7], where analytical expressions for the distribution of the L-values in QAM were presented. Combining them with a generalized transfer function of a code [8], [9] allows us to develop union bounds for the coded BER and to compare the system performance of BICM with different interleavers. In particular, we compare the results of BICM with modular interleavers (BICM-MD) with those obtained using the random interleaver (BICM-RN) of [2] quantifying the achievable improvements when an optimal bit assignment is used. Although previous works we cited noted the influence of the interleaver design and also the effect of mapping, to the best of our knowledge, this paper is the first to analyze formally the interleaver design for BICM transmissions; this is its main contribution.

In this work low complexity BICM receivers are analyzed. Thus, we do not address design issues of BICM with iterative detection/decoding which appear when strong codes (e.g., turbo or LDPC codes) are used, or when BICM itself is treated as a serial concatenation of the channel encoder and the modulator. For the latter case, abundant literature exists which discusses the design of bit mappings for improving the system performance in the waterfall or the error-floor region [10]–[12]. Simple BICM schemes analyzed in this paper are used in delay constrained systems, for example in control information blocks as proposed by the WINNER project [13]. Other application examples include the low complexity receivers proposed by the IEEE for the multiband OFDM ultra wide-band transceivers [14].

The paper is organized as follows. We introduce the model of the system in Section II. The interleaver design is analyzed in Section III. In Section IV we present the numerical results. Finally, in Section V the conclusions are drawn.

Research supported by the Swedish Research Council, Sweden (under research grant #2006-5599), and by NSERC, Canada (under research grant #249704-07).

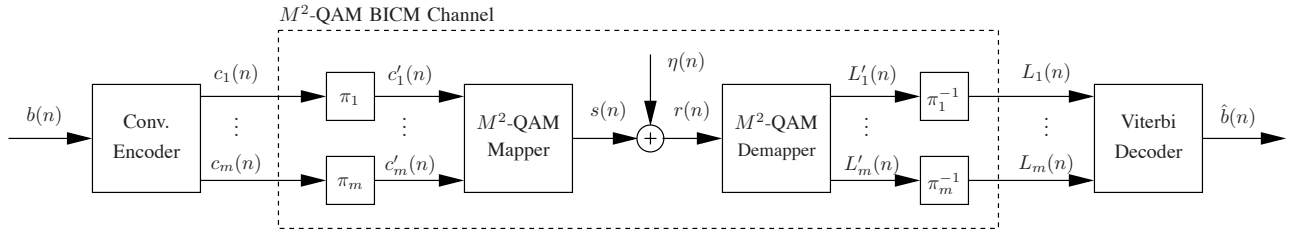


Fig. 1. Model of BICM with modular interleavers: a convolutional encoder followed by  $m$  interleavers ( $\pi_1, \dots, \pi_m$ ), the  $M^2$ -QAM mapper ( $\mathcal{M}$ ), an AWGN channel, the demapper ( $\mathcal{M}^{-1}$ ), the interleaved metrics, the deinterleavers and the Viterbi Decoder.

## II. SYSTEM MODEL

The model of BICM-MD is shown in Fig. 1. The information bits  $b(n)$  are encoded by a feedforward convolutional encoder with rate  $R = 1/m$ . The encoder is defined by the polynomial generators  $(g_1, \dots, g_m)$  each of them producing the coded bits  $c_k(n)$  which are gathered in codewords  $\mathbf{c}(n) = [c_1(n), \dots, c_m(n)]$  (as a notational convention, boldface symbols denote vectors). These bits are further independently permuted into  $\mathbf{c}'(n)$  by ideal (infinite depth) independent interleavers  $\pi_k, k = 1, \dots, m$ .

The coded and interleaved bits  $\mathbf{c}'(n)$  are mapped to  $M^2$ -QAM symbols using a memoryless mapping  $\mathcal{M} : \{0, 1\}^m \rightarrow \mathcal{X}$ , where  $\mathcal{X} = \{a_1, \dots, a_M\}$  is an  $M$ -level pulse amplitude modulation (PAM) constellation with  $M = 2^m$ . The mapping considered here is based on the so-called binary reflected Gray code (BRGC) [15]. Consequently, the  $M^2$ -QAM constellation is formed by the direct product of two  $M$ -PAM constellations. The symbols from  $\mathcal{X}$  are defined as  $a_l = (2l - 1 - M)\Delta$  with  $l = 1, \dots, M$ , where  $2\Delta$  is the minimum distance between the constellation symbols. The constellation is normalized to average unitary energy so  $\Delta = \sqrt{\frac{3}{2(M^2-1)}}$ .

We define also  $\mathcal{G}_o$  as the  $o$ -th enumeration order of the polynomials generators  $(g_1, \dots, g_m)$  where  $o = 1, \dots, m!$ . The need for this notation will become clear after Section III where  $\mathcal{G}_o$  will be an element of the optimization space.

The result of the transmission is given by  $r(n) = s(n) + \eta(n)$ , where  $\eta \in \mathbb{R}$  is a zero-mean, real, white Gaussian noise with variance  $N_0/2$ . The average signal-to-noise ratio (SNR) per complex symbol is given by  $\gamma = \frac{1}{N_0}$ . On the receiver side, the reliability metrics of the transmitted bits are calculated under the form of logarithmic likelihood ratios (L-values) for each bit position. The soft information  $\mathbf{L}'(n)$  is deinterleaved and then passed to a Viterbi decoder which produces an estimation of the transmitted bit  $\hat{b}(n)$ . We consider here the case where the number of the encoder's outputs is equal to the number of bits in the real/imaginary parts of the QAM symbols. However, the analytical framework we develop will also allow us to study other cases.

In this paper we are interested in low complexity BICM schemes and therefore a convolutional code is used. Analysis of more complex implementations such as BICM with iterative decoding or BICM with capacity approaching codes are out of the scope of this paper. We also emphasize that the proposed scheme is different from the so-called multi-level coding

(MLC) [16] through the fact that only one encoder is present in the system. That is, each of the independently interleaved coded bits carries information about the same information bits, as opposed to MLC, where multiple encoders are related to independent streams of information bits.

### A. Equivalent Channel Models

Using the results presented in [7] it is possible to build an equivalent model for the  $M^2$ -QAM BICM Channel shown in Fig. 1. In this model each of the bits can be seen as bits sent using binary phase shift keying (BPSK) over a *virtual AWGN channel* with different SNR. Then the L-values  $L_k(n)$  can be modeled as random Gaussian variables with the same variance but with means which depends on both the transmitted symbol (i.e., not only the bit's value but also the value of its neighbors in the codeword) and the bit's position. Alternative models where both the variance and the mean are changing were shown to be less accurate. In fact, the approximation whose principles we shortly outline here yields accurate approximation of the distribution of the L-values in the vicinity of zero (for more details see [7], [17], [18]).

Due to the properties of BRGC, symbols with the  $k$ -th bit set to  $b$  are clustered so that the closest symbol with the opposite value of the bit at the position  $k$ , may be at a distance that varies from  $2\Delta$  to  $2\Delta \cdot \frac{M}{2^k}$ . That is, when  $k = m$ , there is always an adjacent symbol (at distance  $2\Delta$ ) with the opposite value of the bit. On the other hand, for  $k = 1$ , the number of possible distances grows to  $M/2$ . This effect is sometimes referred as "protection" experienced by the bits, which depends on their position. For  $k = m$  the bits have always the same "low" protection but for  $k = 1$ , depending on the value of other bits in the modulating codeword, the protection may be relatively high.

This effect is reflected in the distribution of the L-values that changes depending on the sent symbol. It is possible to model this phenomenon using a Gaussian distribution whose variance  $\sigma^2$  depends uniquely on the SNR, but whose mean  $\mu_j$  depends also on the distance of the sent symbol to the closest symbol with the opposite bit. Consequently, the L-values can be modeled as

$$L_k(n) \sim \mathcal{N}(\mu_j, \sigma^2), \quad (1)$$

where  $\mathcal{N}(a, b)$  is a Gaussian distribution with mean value  $a$

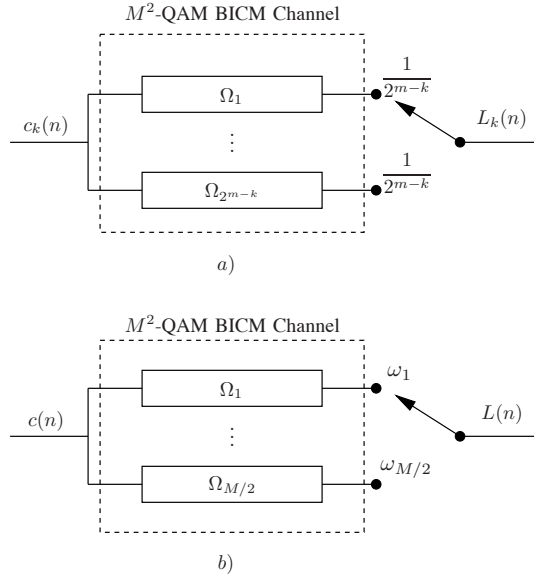


Fig. 2. Equivalent channel models for the  $M^2$ -QAM Channel: a) MD interleaver and b) RN interleaver

and variance  $b$ , and

$$\mu_j = 4\gamma\Delta^2(2j - 1) \quad (2)$$

$$\sigma^2 = 8\gamma\Delta^2, \quad (3)$$

with  $j = 1, \dots, M/2$ .

According to (1), (2), and (3), there are  $M/2$  different Gaussian distributions that can be used to model the L-values. We define a virtual channel  $\Omega_j$  as an AWGN channel with parameters  $(\mu_j, \sigma^2)$ .

For the general case of an MD interleaver, we define  $\rho_{k,j}$  as the probability that a bit at position  $k$  passes through  $\Omega_j$ . It is given by

$$\rho_{k,j} = \begin{cases} \frac{1}{2^{m-k}} & \text{if } j = 1, \dots, 2^{m-k} \\ 0 & \text{if } j = 2^{m-k} + 1, \dots, \frac{M}{2} \end{cases}, \quad (4)$$

that is,  $\Omega_1$  can be used by the bit for all positions  $k$ ,  $\Omega_2$  only for  $k \leq m - 1$ ,  $\Omega_3$  and  $\Omega_4$  only for  $k \leq m - 2$ ,  $\Omega_5, \dots, \Omega_8$  for  $k \leq m - 3$ , and so on.

If instead we consider the standard RN interleaver, we have to average  $\rho_{k,j}$  over the bit's positions. Thus, the probability of selecting the  $j$ -th virtual channel  $\Omega_j$  is given by

$$\begin{aligned} \omega_j &= \frac{1}{m} \sum_{k=1}^m \rho_{k,j} = \frac{2}{m \cdot M} \sum_{k=1}^{m - \lceil \log_2(j) \rceil} 2^{k-1} \\ &= \frac{2(2^{m - \lceil \log_2(j) \rceil} - 1)}{m \cdot M}. \end{aligned} \quad (5)$$

Finally, we can write

$$\Pr\{L_k(n) \sim \mathcal{N}(\mu_j, \sigma^2)\} = \begin{cases} \rho_{k,j} & \text{for BICM-MD} \\ \omega_j & \text{for BICM-RN,} \end{cases} \quad (6)$$

TABLE I

PROBABILITIES OF SELECTING THE DIFFERENT VIRTUAL CHANNELS FOR DIFFERENT BIT POSITIONS FOR BICM-MD, CF. (4).

$k \setminus j$	1	2	3	$\rho_{k,j}$ 4	5	6	7	8
1	1/8	1/8	1/8	1/8	1/8	1/8	1/8	1/8
2	1/4	1/4	1/4	1/4	0	0	0	0
3	1/2	1/2	0	0	0	0	0	0
4	1	0	0	0	0	0	0	0

TABLE II

PROBABILITIES OF SELECTING THE DIFFERENT VIRTUAL CHANNELS BICM-RN, CF. (5).

$j$	1	2	3	4	5	6	7	8
$\omega_j$	15/32	7/32	3/32	3/32	1/32	1/32	1/32	1/32

where the probabilities  $\rho_{k,j}$  and  $\omega_j$  are given by (4) and (5) respectively. The resulting equivalent channel models are schematically shown in Fig. 2.

To clarify these briefly outlined concepts we will use an example. Consider a rate  $R = 1/4$  convolutional code used in conjunction with 256-QAM ( $M = 16$ ). There are 4 bit positions per real/imaginary part, and  $8 = \frac{16}{2}$  virtual AWGN channels with mean values and variances given by (2) and (3) respectively. The probabilities of sending the bit at position  $k$  over the channel  $\Omega_j$  for MD and RN interleavers are shown, respectively, in Table I and Table II.

### III. PERFORMANCE ANALYSIS

#### A. Union Bounds for the Coded BER

Union bound techniques are a very simple method to approximate the coded BER of a convolutional code. In this section we develop union bounds for the BER of BICM-MD and BICM-RN transmission using the equivalent channel models outlined before. The bounds presented in this section are tight for medium/low BER (less than  $10^{-4}$ ); tighter bounds as those presented in [19], [20] might be used to improve the accuracy of the BER estimation.

For any convolutional code it is possible to define a *generalized transfer function* which enumerates not only the number of non-zero output bits over a path, but the *location* of those bits, i.e., it indicates which branch the non-zero outputs are associated with, [1], [8]. Using the notation of [21] we define the generalized transfer function of the code as

$$T(\mathbf{D}, L, I) = \sum_{\mathbf{d}, l, i} T_{d_1, \dots, d_n, l, i} D_1^{d_1} \dots D_n^{d_n} L^l I^i, \quad (7)$$

where the generalized weight distribution  $\mathbf{d} = (d_1, \dots, d_n)$  denotes the weights of each output of the encoder, and  $\mathbf{D} = (D_1, \dots, D_n)$ ,  $L$ , and  $I$  are dummy variables.  $T_{d_1, \dots, d_n, l, i}$  denotes the number of paths diverging from the zero state and merging with the zero state after  $l$  steps, associated with an input sequence of weight  $i$  and an output sequence of generalized weight  $\mathbf{d}$ .

Once the transfer function of the code is determined, the bit weight enumerating function (WEF) can be calculated as

$$B(\mathbf{D}) = \left. \frac{\partial T(\mathbf{D}, L, I)}{\partial I} \right|_{I=L=1}. \quad (8)$$

Based on the generalized bit WEF  $B(\mathbf{D})$ , it is possible to compute the weight distribution spectrum of the code taking into account not only the number of errors (classic approach) but the location of those errors. The values of this  $m$ -dimensional weight distribution spectrum can be extracted directly from from (8) as

$$\beta(\mathbf{d}) = \frac{1}{\prod_{k=1}^m d_k!} \cdot \left. \frac{\partial B(\mathbf{D})}{\partial D_1^{d_1} \dots \partial D_m^{d_m}} \right|_{\mathbf{D}=\mathbf{0}}. \quad (9)$$

Using this weight distribution spectrum, the union bound (UB) on the BER is given by

$$P_b \leq \text{UB} = \sum_{\mathbf{d}} \beta(\mathbf{d}) \cdot \text{PEP}(\mathbf{d}), \quad (10)$$

where  $\text{PEP}(\mathbf{d})$  is the pairwise error probability which represents the probability of detecting a codeword with Hamming weight  $\mathbf{d}$  instead of the transmitted all-zero codeword.

Equation (10) is the generalization of the conventional union bound [21, Ch. 5] which can be obtained by setting  $D_i = D \forall i$  and  $d_1 + d_2 + \dots + d_n = d$ .

### B. Interleaver Structure

We introduce the variable  $u_{k,j}$  which denotes the number of bits among  $\mathbf{d}$  that used  $\Omega_j$  in the bit position  $k$ . We also introduce  $v_j$  which denotes the number of bits that used  $\Omega_j$  added up over all the bit positions. Consequently, the constraints for the different variables are:

$$\sum_{j=1}^{M/2} u_{k,j} = d_k, \quad \sum_{k=1}^m u_{k,j} = v_j. \quad (11)$$

Due to the channel and the infinite depth interleaver, the  $L$ -values are assumed to be independent Gaussian random variables with different mean values and variances. Thus, the sum of these  $\mathbf{d}$  Gaussians will be a new Gaussian random variable. Its mean and variance will be determined based on the number of bits that randomly were transmitted through the different  $\Omega_j$  channels. Thus, the conditional pairwise error probability of selecting a wrong path of length  $\mathbf{d}$  is given by

$$\text{PEP}(\mathbf{d}|\mathbf{v}) = Q \left( \sum_{j=1}^{M/2} v_j \mu_j / \sqrt{\sigma^2 \sum_{j=1}^{M/2} v_j} \right),$$

where  $Q(x) = \frac{1}{\sqrt{2\pi}} \int_x^\infty \exp(-t^2/2) dt$  and  $\mathbf{v} = (v_1, \dots, v_{M/2})$ .

Conditioning on the number of bits going through the different channels, we have that

$$\begin{aligned} \text{PEP}(\mathbf{d}) &= \sum_{\mathbf{v}} \text{PEP}(\mathbf{d}|\mathbf{v}) \cdot \text{Prob}\{\mathbf{v}\} \\ &= \sum_{\mathbf{v}} \text{PEP}(\mathbf{d}|\mathbf{v}) \cdot \sum_{\mathbf{U}} \text{Prob}\{\mathbf{v}|\mathbf{U}\} \cdot \text{Prob}\{\mathbf{U}\}, \end{aligned} \quad (12)$$

where  $\sum_{\mathbf{u}} \text{Prob}\{\mathbf{v}|\mathbf{u}\} \cdot \text{Prob}\{\mathbf{u}\}$  has to be computed for the different interleaver configurations and  $\mathbf{U}$  is a matrix containing the elements  $u_{k,j}$ .

1) *Modular Interleaver*: In this case,

$$\sum_{\mathbf{U}} \text{Prob}\{\mathbf{v}|\mathbf{U}\} \cdot \text{Prob}\{\mathbf{U}\} = \sum_{\mathbf{U}} \prod_{k=1}^m d_k! \prod_{j=1}^{M/2} \frac{\rho_{k,j}^{u_{k,j}}}{u_{k,j}!}, \quad (13)$$

and thus

$$\begin{aligned} P_b^{\text{MD}}(\mathcal{G}_o) &\leq \sum_{\mathbf{d}} \beta(\mathbf{d}) \sum_{\mathbf{v}} Q \left( \sum_{j=1}^{M/2} v_j \mu_j / \sqrt{\sigma^2 \sum_{j=1}^{M/2} v_j} \right) \cdot \\ &\quad \sum_{\mathbf{U}} \prod_{k=1}^m d_k! \prod_{j=1}^{M/2} \frac{\rho_{k,j}^{u_{k,j}}}{u_{k,j}!}. \end{aligned} \quad (14)$$

Note that in (14) we emphasize the fact that the BER depends on the enumerating order  $\mathcal{G}_o$ .

2) *Random Interleaver*: In this case,

$$\sum_{\mathbf{U}} \text{Prob}\{\mathbf{v}|\mathbf{U}\} \cdot \text{Prob}\{\mathbf{U}\} = d! \prod_{j=1}^{M/2} \frac{\omega_j^{v_j}}{v_j!}, \quad (15)$$

and consequently

$$\begin{aligned} P_b^{\text{RN}} &\leq \sum_{\mathbf{d}} \beta(\mathbf{d}) \sum_{\mathbf{v}} Q \left( \sum_{j=1}^{M/2} v_j \mu_j / \sqrt{\sigma^2 \sum_{j=1}^{M/2} v_j} \right) \cdot \\ &\quad d! \prod_{j=1}^{M/2} \frac{\omega_j^{v_j}}{v_j!}. \end{aligned} \quad (16)$$

Note that in this case, the bound does not depend on the polynomial order (although it obviously depends on the set of polynomial generators).

### C. Simplifications

Equation (14) contains three summations which may be tedious to evaluate, specially when the size of the constellation is large. In order to efficiently compute the bound, in this section we propose to use only a reduced part of the whole weight distribution spectrum  $\beta(\mathbf{d})$ .

First note that the summations in (14) were presented in the following order:  $\mathbf{d}$ ,  $\mathbf{v}$  and  $\mathbf{U}$ . This order was selected to clarify the developments, however, we note that it is possible to suitably invert the order of the summations, i.e., instead of implementing the three group of summations in (14), it is possible carry out the summations starting from  $\mathbf{U}$ . For a given  $\mathbf{U}$ ,  $\mathbf{d}$  and  $\mathbf{v}$  can be calculated from (11).

Using this approach, the bound for BICM-MD case can be rewritten as

$$\begin{aligned} P_b^{\text{MD}}(\mathcal{G}_o) &\leq \sum_{\mathbf{U}} \beta(\mathbf{d}) \cdot Q \left( \sum_{j=1}^{M/2} v_j \mu_j / \sqrt{\sigma^2 \sum_{j=1}^{M/2} v_j} \right) \cdot \\ &\quad \prod_{k=1}^m d_k! \prod_{j=1}^{M/2} \frac{\rho_{k,j}^{u_{k,j}}}{u_{k,j}!}, \end{aligned} \quad (17)$$

where  $d_k$  and  $v_j$  are given by (11).

Additionally, it is necessary to restrict the values of  $\mathbf{d}$  to be considered. For all the numerical examples presented in Section IV we carry out the summation in (17) for all the values of  $\mathbf{U}$  such that

$$d_f \leq \sum_{k=1}^m d_k \leq d_f + 4. \quad (18)$$

where  $d_f$  is the free distance of the code.

We selected  $d_f + 4$  since no notable improvement in the accuracy of approximation of the true value of the UB was observed beyond this limit.

#### IV. NUMERICAL EXAMPLES

As mentioned before the performance of BICM-MD depends on the enumeration of the polynomial generators  $\mathcal{G}_o$ . Thus, the optimal bit assignment problem can be seen as the problem of finding the optimum enumeration order among the  $m!$  candidates.

For a given  $\gamma$  it is possible to find the optimal enumeration order. However, it is more practical to compare the performance for a common target BER ( $\text{BER}_0$ ). Setting  $\gamma$  such that BER is close to  $\text{BER}_0$  is sufficient in practice, i.e., the optimal enumeration order stays constant in a very large band of  $\gamma$ .

We define  $\hat{\mathcal{G}}$  as the enumerating order that minimizes the SNR needed to reach  $\text{BER}_0$ , and  $\gamma_0^{\hat{\mathcal{G}}}$  as the value of SNR that produces  $\text{BER}_0$ . Analogously,  $\check{\mathcal{G}}$  is defined as the enumeration order that maximizes the SNR for a given  $\text{BER}_0$ , i.e., the “worst” bit assignment. We also introduce the variables  $\gamma_0^{\check{\mathcal{G}}}$ , and  $\gamma_0^{\text{RN}}$  which represent the value of SNR that the last two different configuration need to reach  $\text{BER}_0$ .

For all the simulations presented in this section, the optimum distance spectrum (ODS) codes [22] were used. However, we note that the optimality of these codes for BICM-MD has not been yet proven. This issue is out of the scope of this paper and remains as a problem to be further investigated.

For all the results presented below, the optimization of the enumerating orders was carried out for  $\text{BER}_0 = 10^{-6}$ . Additionally, in order to efficiently compute the values of the bit WEFs, the recursive algorithm proposed in [23] was used.

##### A. BICM 16-QAM and $R = 1/2$

For 16-QAM there are only two channels  $\Omega_1$  and  $\Omega_2$ , and the probabilities associated are [cf. (4) and (5)]

$$\begin{aligned} \rho_{1,1} = \rho_{1,2} = 0.5, \rho_{2,1} = 1, \rho_{2,2} = 0 \\ \omega_1 = 0.75, \omega_2 = 0.25 \end{aligned}$$

Since  $R = 1/2$ , two enumeration orders  $\mathcal{G}_o$  are possible: either  $\mathcal{G}_1 = (g_1, g_2)$  or  $\mathcal{G}_2 = (g_2, g_1)$ .

The UB for BICM-MD in this case is given by

$$\begin{aligned} \text{UB} \approx \sum_{u_{1,1}=0}^{\infty} \sum_{u_{2,1}=0}^{\infty} \sum_{u_{1,2}=0}^{\infty} \sum_{u_{2,2}=0}^{\infty} \beta(d_1, d_2) \mathcal{I}_{[d_f \leq d \leq d_f+4]} \cdot \\ Q \left( \frac{v_1 \mu_1 + v_2 \mu_2}{\sigma \sqrt{v_1 + v_2}} \right) \cdot \prod_{k=1}^2 d_k! \prod_{j=1}^2 \frac{\rho_{k,j}^{u_{k,j}}}{u_{k,j}!}, \quad (19) \end{aligned}$$

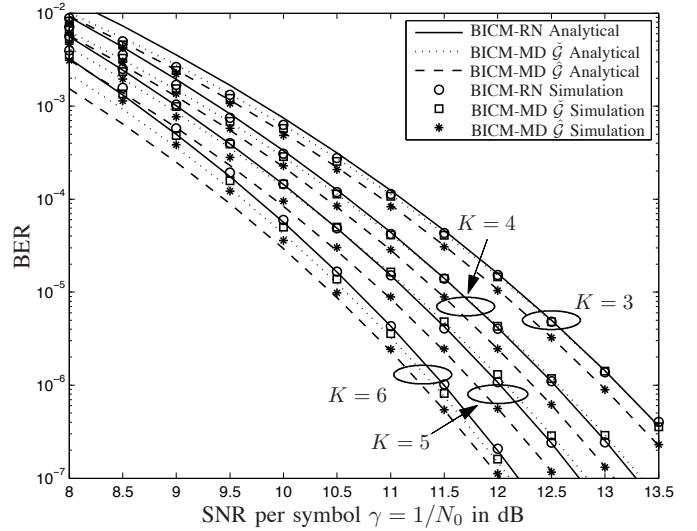


Fig. 3. BER for the convolutional codes for BICM-RN (circles), BICM-MD (asterisks and squares for  $\hat{\mathcal{G}}$  and  $\check{\mathcal{G}}$  respectively), and the bounds for RN (solid lines) and MD (dashed and dotted lines) for 16-QAM and  $R = 1/2$ .

TABLE III  
OPTIMUM BIT ASSIGNMENTS FOR BICM-MD WITH  $R = 1/2$  AND 16-QAM FOR  $\text{BER}_0 = 10^{-6}$ .

$K$	$\hat{\mathcal{G}}$	$\check{\mathcal{G}}$	$\gamma_0^{\check{\mathcal{G}}} - \gamma_0^{\hat{\mathcal{G}}}$	$\gamma_0^{\text{RN}} - \gamma_0^{\hat{\mathcal{G}}}$
3	(7,5)	(5,7)	0.16 dB	0.16 dB
4	(15,17)	(17,15)	0.23 dB	0.20 dB
5	(23,35)	(35,23)	0.26 dB	0.22 dB
6	(75,53)	(53,75)	0.11 dB	0.21 dB

where  $d_k$  and  $v_j$  are given by (11). Here we added an indicator function  $\mathcal{I}_{[S]}$  which is one if  $S$  is true, and zero if  $S$  is false. Note also that the sign  $\approx$  is used to emphasize the fact that due to (18), (19) is an approximation rather than an upper bound.

For BICM-RN the UB on the BER is given by

$$\text{UB} \approx \sum_{d=d_f}^{d_f+4} \beta(d) \sum_{v_1=0}^d Q \left( \frac{v_1 \mu_1 + v_2 \mu_2}{\sigma \sqrt{v_1 + v_2}} \right) d! \prod_{j=1}^2 \frac{\omega_j^{v_j}}{v_j!}, \quad (20)$$

where  $v_2 = d - v_1$ .

In Fig. 3 we present the numerical results obtained for different constraint lengths, contrasting them with the results obtained through numerical simulations. We used ODS codes with generating polynomials (5, 7), (15, 17), (23, 35), and (53, 75) for  $K = 3, 4, 5$  and 6 respectively (all the polynomials are given in octal notation). The summary with the optimum bit assignments in this case is shown in Table III.

##### B. BICM 64-QAM and $R = 1/3$

We again use ODS codes, i.e., (5,7,7), (13,15,17) and (25,33,37) for  $K = 3, 4$  and 5 respectively. Now, there are 8 virtual channels, 3 bit positions, and for each value of  $K$ , there are  $3! = 6$  different possible enumeration orders. We refrain from showing the explicit form of (14) and (16) not to overcrowd the paper with equations.

TABLE IV  
OPTIMUM BIT ASSIGNMENTS FOR BICM-MD WITH  $R = 1/3$  AND  
64-QAM FOR  $BER_0 = 10^{-6}$ .

$K$	$\hat{\mathcal{G}}$	$\tilde{\mathcal{G}}$	$\gamma_0^{\hat{\mathcal{G}}} - \gamma_0^{\tilde{\mathcal{G}}}$	$\gamma_0^{\text{RN}} - \gamma_0^{\hat{\mathcal{G}}}$
3	(5,7,7)	(7,7,5)	0.75 dB	0.75 dB
4	(15,17,13)	(17,15,13)	0.23 dB	0.72 dB
5	(25,33,37)	(37,33,25)	0.32 dB	0.63 dB

Searching for the bit assignment, the optimum polynomial order was found for each constraint length. In Table IV the optimal enumeration orders found are presented together with the improvements compared with both BICM-RN, and BICM-MD with the worst enumeration order. In Fig. 4 the BER curves are shown.

Analyzing the results presented in Fig. 3, Fig. 4, and Tables III and IV, we can draw the following conclusions

- BICM-MD using the optimum enumeration order always outperforms BICM-RN. For the analyzed cases, these improvements can be up to 0.75 dB for  $BER_0 = 10^{-6}$ . Moreover, we note that the achievable improvements strongly depend on the target BER. For example, for  $R = 1/3$ , 64-QAM,  $K = 3$  and for a  $BER_0 = 10^{-3}$ , the improvements are up to 1.7 dB!
- BICM-MD with the worst enumeration can degrade the system performance compared with BICM-RN (cf. Fig. 3 for  $K = 5$ ). Thus, deciding to use the modular interleavers optimization of the enumeration order  $\mathcal{G}_o$  is a must.
- On the other hand, BICM-MD with the worst enumeration order can outperform the RN interleaver (cf.  $K = 6$  Fig. 3 and  $K = 4, 5$  in Fig. 4). Consequently, BICM-RN cannot be, in general, considered as a “conservative” solution in between the “best” and the “worst” enumeration order of BICM-MD.

We emphasize that the developed bounds are asymptotically tight and match the simulated performance for BER less than  $10^{-4}$  (cf. Fig. 3 and Fig. 4). For all the studied cases, only a relatively small number of enumeration orders had to be tested, yet to obtain the BER points heavy numerical simulations were needed. On the other hand, the bounds developed are ready-to-use formulas and their run-time is negligible comparing to the simulations.

Finally we recall the fact that in order to improve the system performance using BICM-MD, the optimization of the bit’s assignments (i.e., the enumeration order) is a mandatory step; skipping it can degrade the performance when comparing to BICM-RN.

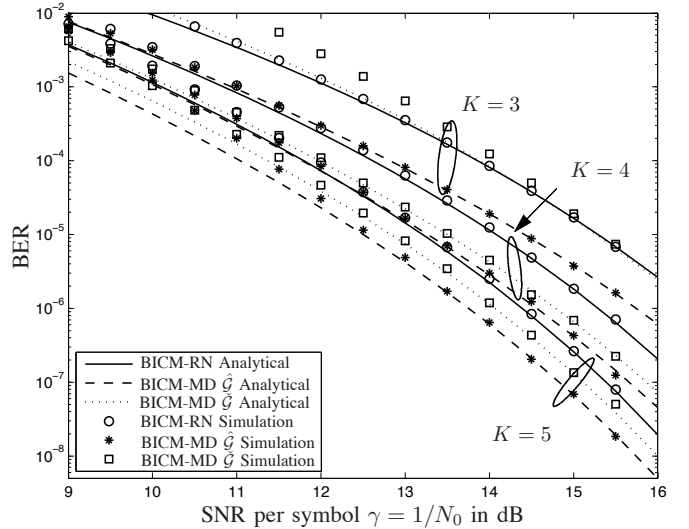


Fig. 4. Simulated BER for the convolutional codes for BICM-RN (circles), BICM-MD (asterisks and squares for  $\hat{\mathcal{G}}$  and  $\tilde{\mathcal{G}}$  respectively) and the bounds for BICM-RN (solid lines) and BICM-MD (dashed and dotted lines) for 64-QAM and  $R = 1/3$ .

## V. CONCLUSIONS AND FUTURE WORK

In this paper we analyzed and designed the so-called modular interleavers for BICM transmissions. We developed analytical bounds for the coded BER and we showed that using a proper bit assignment of the output bits of the encoder to the  $M^2$ -QAM symbol, it is possible to improve the performance of the system when comparing to the “conventional” (unstructured) interleaver design. Moreover, we showed that a suboptimal bit assignment could in fact degrade the performance of the system.

The analytical framework we established and the results we presented point to some sources of sub-optimality of the unstructured design of the BICM transmitters. First of all, the convolutional codes that are commonly used are those whose performance is optimized for BPSK transmission over AWGN channels. It might then be possible to design codes that are optimized to operate with high-order modulation schemes (such as  $M^2$ -QAM). Secondly, the assignment between the encoder’s output and the modulator input we explored, has more dimensions, in general related to the case when the number of coded output bits and the modulator input bits do not match. The relationship between such cases and the search for optimal codes is another open question. These issues are left for further investigation.

## ACKNOWLEDGMENT

The authors thank Mr. A. Ceron (UTFSM, Chile) for the numerical implementation of the recursive algorithm [23] to compute the weight distribution spectrum of the code.

## REFERENCES

- [1] E. Zehavi, "8-PSK trellis codes for a Rayleigh channel," *IEEE Trans. Commun.*, vol. 40, no. 3, pp. 873–884, May 1992.
- [2] G. Caire, G. Taricco, and E. Biglieri, "Bit-interleaved coded modulation," *IEEE Trans. Inform. Theory*, vol. 44, no. 3, pp. 927–946, May 1998.
- [3] X. Li and J. A. Ritcey, "Bit-interleaved coded modulation with iterative decoding," *IEEE Commun. Lett.*, vol. 1, no. 6, pp. 169–171, Nov. 1997.
- [4] A. Nilsson and T. M. Aulin, "On in-line bit interleaving for serially concatenated systems," in *International Conference on Communications ICC 2005*, vol. 1, May 2005, pp. 547–552.
- [5] E. Rosnes and Ø. Ytrehus, "On the design of bit-interleaved turbo-coded modulation with low error floors," *IEEE Trans. Commun.*, vol. 54, no. 9, pp. 1563–73, Sept. 2006.
- [6] R. D. Maddock and A. H. Banihashemi, "Reliability-based coded modulation with low-density parity-check codes," *IEEE Trans. Commun.*, vol. 54, no. 3, pp. 403–406, Mar. 2006.
- [7] A. Alvarado, L. Szczecinski, R. Feick, and L. Ahumada, "Distribution of L-values in Gray-mapped  $M^2$ -QAM signals: Exact expressions and simple approximations," in *IEEE Global Telecommunications Conference GLOBECOM 2007*, Washington, USA, Nov. 2007.
- [8] X. Li, A. Chindapol, and J. A. Ritcey, "Bit-interlaved coded modulation with iterative decoding and 8PSK signaling," *IEEE Trans. Commun.*, vol. 50, no. 6, pp. 1250–1257, Aug. 2002.
- [9] Y. S. Leung, S. G. Wilson, and J. W. Ketchum, "Multifrequency trellis coding with low delay for fading channels," *IEEE Trans. Commun.*, vol. 41, no. 10, pp. 1450–1459, Oct. 1993.
- [10] M. Tüchler, "Design of serially concatenated systems depending on the block length," *IEEE Trans. Commun.*, vol. 52, no. 2, pp. 209–218, Feb. 2004.
- [11] F. Schreckenbach, N. Görtz, J. Hagenauer, and G. Bauch, "Optimization of symbol mappings for bit-interleaved coded modulation with iterative decoding," *IEEE Commun. Lett.*, vol. 7, no. 12, pp. 593–595, Dec. 2003.
- [12] A. Chindapol and J. A. Ritcey, "Design, analysis, and performance evaluation for BICM-ID with square QAM constellations in Rayleigh fading channels," *IEEE J. Select. Areas Commun.*, vol. 19, no. 5, pp. 944–957, May 2001.
- [13] T. Lestable *et al.*, "D2.2.3 modulation and coding schemes for the WINNER II system," WINNER II, Tech. Rep. IST-4-027756, November 2007, available at <https://www.ist-winner.org>.
- [14] A. Batra *et al.*, "Multi-band OFDM physical layer proposal for IEEE 802.15 task group 3a," Mar. 2004, Document IEEE P802.15-03/268r3, available at <http://grouper.ieee.org/groups/802/15/>.
- [15] E. Agrell, J. Lassing, E. G. Ström, and T. Ottosson, "Gray coding for multilevel constellations in Gaussian noise," *IEEE Trans. Inform. Theory*, vol. 53, no. 1, pp. 224–235, Jan. 2007.
- [16] U. Wachsmann, R. Fischer, and J. B. Huber, "Multilevel codes: Theoretical concepts and practical design rules," *IEEE Trans. Inform. Theory*, vol. 45, no. 5, pp. 1361–1391, Jul. 1999.
- [17] M. Benjillali, L. Szczecinski, S. Aissa, and C. Gonzalez, "Evaluation of bit error rate for packet combining with constellation rearrangement," *Wiley Journal Wireless Comm. and Mob. Comput. (published on-line)*, available at <http://doi.wiley.com/10.1002/wcm.528>, June 2007.
- [18] C. Wengerter, A. von Elbwart, E. Seidel, G. Velev, and M. Schmitt, "Advanced hybrid ARQ technique employing a signal constellation rearrangement," in *IEEE Vehicular Technology Conference 2002, VTC-2002 Fall*, Sept. 2002, pp. 2002–2006.
- [19] H. Kuai, F. Alajaji, and G. Takahara, "Tight error bounds for non-uniform signaling over AWGN channels," *IEEE Trans. Inform. Theory*, vol. 46, no. 7, pp. 2712–2718, Nov. 2000.
- [20] A. Cohen and N. Merhav, "Lower bounds on the error probability of block codes based on improvements on de Caen's inequality," *IEEE Trans. Inform. Theory*, vol. 50, no. 2, pp. 290–310, Feb. 2004.
- [21] A. J. Viterbi and J. K. Omura, *Principles of Digital Communications and Coding*. McGraw-Hill, 1979.
- [22] P. Frenger, P. Orten, and T. Ottosson, "Convolutional codes with optimum distance spectrum," *IEEE Trans. Commun.*, vol. 3, no. 11, pp. 317–319, Nov. 1999.
- [23] D. Divsalar, S. Dolinar, R. J. McEliece, and F. Pollara, "Transfer function bounds on the performance of turbo codes," JPL, Cal. Tech., TDA Progr. Rep. 42-121, Aug. 1995.